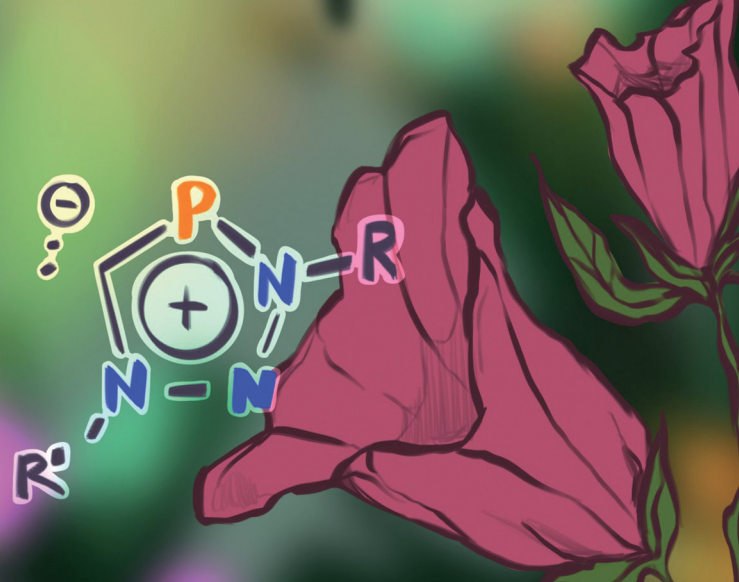


# ChemComm

Chemical Communications

rsc.li/chemcomm



ISSN 1359-7345

## COMMUNICATION

Christian Müller *et al.*

Phosphorus derivatives of mesoionic carbenes: synthesis and characterization of triazaphosphole-5-ylidene →  $\text{BF}_3$  adducts



Cite this: *Chem. Commun.*, 2023,  
59, 10243

Received 6th July 2023,  
Accepted 24th July 2023

DOI: 10.1039/d3cc03268j

rsc.li/chemcomm

# Phosphorus derivatives of mesoionic carbenes: synthesis and characterization of triazaphosphole-5-ylidene $\rightarrow$ $\text{BF}_3$ adducts<sup>††</sup>

Lea Dettling,  <sup>a</sup> Niklas Limberg, <sup>a</sup> Raphaela Küppers, <sup>a</sup> Daniel Frost,  <sup>a</sup> Manuela Weber, <sup>a</sup> Nathan T. Coles,  <sup>b</sup> Diego M. Andrade  <sup>c</sup> and Christian Müller  <sup>a</sup>

Trimethylsilyl-substituted triazaphospholes were synthesized by a [3+2] cycloaddition reaction between organic azides and  $(CH_3)_3Si-C\equiv P$ . In an attempt to isolate their *N*-alkylated products, the formation of  $BF_3$  adducts of unprecedented triazaphosphol-5-ylidenes was found. The nature of the carbon<sub>carbene</sub>–boron bond was investigated within the DFT framework, revealing a strong donation of electrons from the carbene carbon atom to the boron atom combined with weak back-bonding.

According to the isolobal relationship between a trivalent phosphorus atom and a C–H fragment, 3*H*-1,2,3,4-triazaphosphole derivatives **A** are phosphorus analogues of the well-known 1,4-disubstituted 1,2,3-triazoles **B** (Fig. 1), which play a prominent role in the field of “click”-chemistry.<sup>1</sup> These heterocycles possess a high degree of aromaticity and can be obtained in a modular [3+2] cycloaddition reaction, starting from organic azides and phosphalkynes.<sup>2,3</sup>

Although triazaphospholes were first synthesized as early as 1984, reports of their coordination chemistry were first published almost 30 years later.<sup>3,4</sup> Our group reported the coordination chemistry and photoluminescence properties of conjugated, pyridyl-functionalized triazaphospholes, bearing either <sup>1</sup>Bu or Si(CH<sub>3</sub>)<sub>3</sub>-substituents at the 5-position of the heterocycle.<sup>5</sup>

Little is known about the chemical reactivity of triazaphospholes. In addition to our observation that they undergo cyclo-addition-cycloreversion reactions with  $\text{CF}_3\text{C}\equiv\text{CCF}_3$  forming C, we found that triazaphospholenium salts D are accessible by

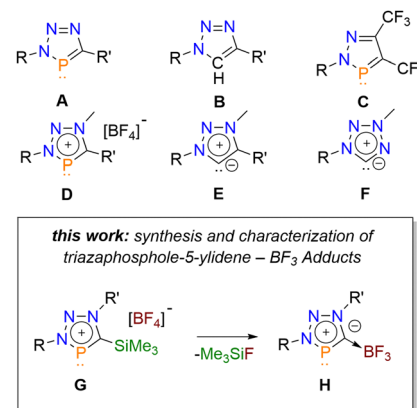


**Fig. 1** Selected phosphorus and nitrogen based heterocycles and brief summary of this work ( $R/R'$ : alkyl- aryl-group)

alkylation of triazaphospholes with Meerwein salts.<sup>6,7</sup> Because a negatively charged carbon atom is valence isoelectronic to a phosphorus atom, these cationic phosphorus heterocycles are formally phosphorus congeners of the well-known mesoionic 1,2,3-triazolylidenes **E** and show an interesting coordination chemistry.<sup>7,8</sup>

Inspired by our recent investigations on 6-membered, 2-Si(CH<sub>3</sub>)<sub>3</sub>-substituted aromatic phosphorus heterocycles (phosphinines), we became interested in reinvestigating Si(CH<sub>3</sub>)<sub>3</sub>-substituted triazaphospholes (**A**,  $R' = \text{Si}(\text{CH}_3)_3$ ), particularly with respect to the formation of the corresponding triazaphospholenium salts (**D**,  $R' = \text{Si}(\text{CH}_3)_3$ ).<sup>5,9</sup> As Si(CH<sub>3</sub>)<sub>3</sub>-groups linked to an aromatic system generally provide interesting electronic effects to the aromatic ring, we anticipated that these compounds might also undergo chemical transformations, such as protodesilylations or C-Si bond cleavage reactions.<sup>10</sup>

Much to our surprise, we now found that  $\text{BF}_4^-$ -salts of  $\text{Si}(\text{CH}_3)_3$ -substituted triazaphospholenium cations (**G**) undergo elimination of  $\text{FSi}(\text{CH}_3)_3$  to form selectively  $\text{BF}_3$  adducts of unprecedented triazaphosphol-5-ylidenes (**H**). Interestingly,

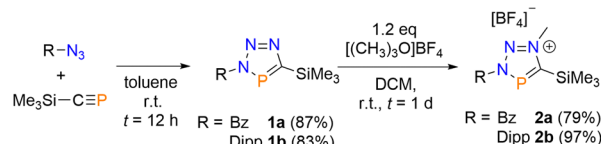
<sup>a</sup>Freie Universität Berlin, Institute of Chemistry and Biochemistry, Fabeckstr. 34/36, Berlin 14195, Germany. E-mail: c.mueller@fu-berlin.de

<sup>b</sup> School of Chemistry, University of Nottingham, University Park, Nottingham NG7 2RD, UK

<sup>c</sup> Universität des Saarlandes, Anorganische Chemie, Saarbrücken 66123, Germany

† Dedicated to Prof. Peter Jutzi on the occasion of his 85<sup>th</sup> birthday.

‡ Electronic supplementary information (ESI) available. CCDC 2279453–2279457. For ESI and crystallographic data in CIF or other electronic format see DOI: <https://doi.org/10.1039/d3cc03268j>

Scheme 1 Synthesis of the triazaphospholenium salts **2a/2b**.

these heterocycles are the phosphorus congeners of tetrazol-5-ylidene carbenes (**F**) with an abnormal substitution pattern.<sup>11</sup>

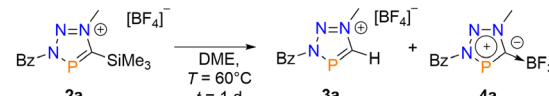
The  $\text{Si}(\text{CH}_3)_3$ -substituted triazaphospholes **1a/b** were synthesized by [3+2] cycloaddition reactions from  $\text{Si}(\text{CH}_3)_3\text{-C}\equiv\text{P}$  and benzyl azide ( $\text{Bz-N}_3$ ) or diisopropylphenyl azide ( $\text{Dipp-N}_3$ ), respectively in good yields (**1a**: 87%, **1b**: 83%, Scheme 1). As expected, both compounds show resonances in the down-field region of the  $^{31}\text{P}\{^1\text{H}\}$  NMR spectrum, at  $\delta(\text{ppm}) = 214.8$  (**1a**) and  $\delta(\text{ppm}) = 222.9$  (**1b**).

Subsequently, we intended to convert **1a/b** into the corresponding  $\text{Si}(\text{CH}_3)_3$ -substituted triazaphospholenium salts of type **G** (Fig. 1). Using an analogous methodology to that of the  $^t\text{Bu}$ -substituted derivatives, an equimolar mixture of compound **1a** and  $[\text{Me}_3\text{O}]^{\text{BF}_4^-}$  was vigorously stirred in dichloromethane at  $T = 55\text{ }^\circ\text{C}$  and the course of the reaction was followed by means of  $^{31}\text{P}\{^1\text{H}\}$  NMR spectroscopy (Fig. S1, ESI<sup>†</sup>). After one hour, the formation of a new species was observed, which we attribute to the desired alkylated triazaphospholenium salt **2a**, due to its characteristic chemical shift at  $\delta(\text{ppm}) = 239.3$ .

However, considerable amounts of starting material were still present, while longer reaction times led to the formation of two more side-products. With the aim of preventing the formation of any side-products,  $[\text{Me}_3\text{O}]^{\text{BF}_4^-}$  was used in a slight excess and the reaction was kept at room temperature. After one day, **2a** was obtained as the sole product in an isolated yield of 79% (Scheme 1). Similarly, the triazaphospholenium salt **2b** was obtained in 97% isolated yield after washing the product with dry diethyl ether. **2b** shows a resonance at  $\delta(\text{ppm}) = 249.1$  in the  $^{31}\text{P}\{^1\text{H}\}$  NMR spectrum. In the  $^1\text{H}$  NMR spectrum of the triazaphospholenium salts, the introduced  $\text{CH}_3$ -group can be detected as a characteristic singlet at  $\delta(\text{ppm}) = 4.52$  (**2a**) and  $\delta(\text{ppm}) = 4.69$  (**2b**), respectively.

Even though the  $\text{Si}(\text{CH}_3)_3$ -substituted triazaphospholenium salts **2a/b** were finally synthesized in high yields, we were still wondering about the formation of the observed side products (*vide supra*), particularly at higher reaction temperatures. Consequently, we investigated the thermal stability of **2a** by heating a solution of this compound in dimethoxyethane (DME) to  $T = 60\text{ }^\circ\text{C}$ . Interestingly, the complete conversion of **2a** to two new species (**3a**, **4a**) was observed by  $^{31}\text{P}\{^1\text{H}\}$  spectroscopy after one day.

We were able to separate both compounds by means of either extraction (**3a**) or flash column chromatography (**4a**). Compound **3a** shows a resonance at  $\delta(\text{ppm}) = 206.7$  in the  $^{31}\text{P}\{^1\text{H}\}$  NMR spectrum, which corresponds to a chemical shift difference of  $\Delta\delta = 32.6$  ppm compared to the starting material **2a** ( $\delta(\text{ppm}) = 239.3$ ). Interestingly, a new signal can be observed in the  $^1\text{H}$  NMR spectrum at  $\delta(\text{ppm}) = 9.26$ . This resonance appears as a doublet with a coupling constant of

Scheme 2 Formation of **3a** and **4a** upon heating of **2a** in DME.

$^2J_{\text{H-P}} = 37.5$  Hz, which is typical of protons in the  $\alpha$ -position to a phosphorus atom. We therefore concluded that **3a** must have been formed by protodesilylation of **2a**, according to Scheme 2. The crystallographic characterization of **3a** indeed confirmed that protodesilylation of **2a** had occurred (Table S1, ESI<sup>†</sup>). Note, that the access to this compound would otherwise only be possible by cycloaddition reaction between an azide and hydrogen cyaphide ( $\text{H-C}\equiv\text{P}$ ), or the cyaphido ligand ( $\text{C}\equiv\text{P}^-$ ), followed by a subsequent quaternization with Meerwein salt.<sup>12</sup>

Up to this point, the source of the proton still remains unknown. It should be noted, however, that protonated side-products have also been observed in the thermal degradation of free 1,2,3-triazol-5-ylidenes.<sup>13</sup>

Next, we turned our attention to the identification of the second species **4a**. Surprisingly, this compound shows a quartet in the  $^{19}\text{F}\{^{31}\text{P}\}$  NMR spectrum at  $\delta(\text{ppm}) = -140.5$  ( $\text{q}$ ,  $^1J_{\text{F-B}} = 37.7$  Hz, Fig. S2, ESI<sup>†</sup>). Likewise, a quartet of doublets is observed in the corresponding  $^{11}\text{B}$  NMR spectrum at  $\delta(\text{ppm}) = 0.6$  ( $\text{d}$ ,  $^2J_{\text{B-P}} = 15.9$  Hz,  $\text{q}$ ,  $^1J_{\text{B-F}} = 37.9$  Hz). The chemical shifts and the coupling pattern is in line with the presence of a  $\text{BF}_3^-$ -carbene adduct. For instance, the classical Arduengo carbene adduct  $\text{IMes} \rightarrow \text{BF}_3$  ( $\text{IMes} = 1,3\text{-dimesitylimidazol-2-ylidene}$ ) shows a resonance in the  $^{19}\text{F}$  NMR spectrum at  $\delta(\text{ppm}) = -142.44$  ( $\text{q}$ ,  $^1J_{\text{F-B}} = 34.6$  Hz) and at  $\delta(\text{ppm}) = -1.36$  ( $\text{q}$ ,  $^1J_{\text{B-F}} = 34.6$  Hz) in the corresponding  $^{11}\text{B}$  NMR spectrum.<sup>15</sup> A coupling to the phosphorus nucleus in **4a** would provide an additional splitting of the otherwise similar signals as can indeed be noticed in the  $^{19}\text{F}$  NMR and the  $^{11}\text{B}$  NMR spectra of **4a** ( $^{19}\text{F}$  NMR:  $\delta(\text{ppm}) = -140.5$  ( $\text{d}$ ,  $^2J_{\text{F-P}} = 14.6$  Hz),  $^{11}\text{B}$  NMR:  $\delta(\text{ppm}) = 0.6$  ppm ( $\text{d}$ ,  $^1J_{\text{B-P}} = 15.9$  Hz), Fig. S2, ESI<sup>†</sup>). Accordingly, the decoupled  $^{11}\text{B}\{^{19}\text{F}\}$  NMR spectrum of **4a** shows only a doublet due to the  $^1J_{\text{B-P}}$  coupling ( $^{11}\text{B}\{^{19}\text{F}\}$  NMR:  $\delta(\text{ppm}) = 0.7$  ( $^1J_{\text{B-P}} = 15.8$  Hz), Fig. S2, ESI<sup>†</sup>). Compound **4b** was synthesized in an analogous manner.

Single crystals of **4a**, suitable for X-ray diffraction, were obtained by layering a concentrated dichloromethane solution of **4a** with *n*-pentane and the molecular structure of **4a**, along with selected bond lengths and distances, is depicted in Fig. 2 (**4b**: Table S3, ESI<sup>†</sup>). The crystallographic characterization of **4a** indeed reveals the presence of an abnormal carbene  $\rightarrow \text{BF}_3^-$ -adduct (Scheme 2). Compared to the protodesilylated triazaphospholenium salt **3a**, the  $\text{P}(1)\text{-C}(1)$  bond in **4a** is slightly elongated (**4a**:  $1.711(2)$  Å; **3a**:  $1.706(2)$  Å), while the  $\text{N}(1)\text{-P}(1)\text{-C}(1)$  bond angle is somewhat larger and closer to  $90^\circ$  (**4a**:  $87.31(8)^\circ$ ; **3a**:  $85.75(6)^\circ$ ). The  $\text{C}(1)\text{-B}(1)$  bond length of  $1.640(3)$  Å is very similar to the one found for the  $\text{C-B}$ -bond distance in the Lewis pairs of classical Arduengo carbenes ( $1.635(5)$  Å for  $\text{IMes} \rightarrow \text{BF}_3$  and  $1.669(6)$  Å for  $4,5\text{-dichloro-IMes} \rightarrow \text{BF}_3$ ).<sup>14</sup> Similar bond lengths and distances were observed also for **4b** (Table S3, ESI<sup>†</sup>). **4a** can be described as a  $\text{BF}_3^-$  adduct of an unprecedented



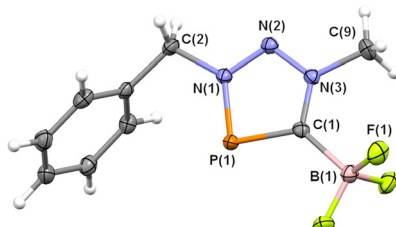


**Fig. 2** Molecular structure of **4a** in the crystal. Displacement ellipsoids are shown at the 50% probability level. Selected experimental and theoretical [B3LYP-D3(BJ)/def2-SVP] bond lengths (Å) and angles (°): P(1)–C(1): 1.711(2) [1.722], P(1)–N(1): 1.705(2) [1.755], N(1)–N(2): 1.309(2) [1.301], N(2)–N(3): 1.320(2) [1.316], N(3)–C(1): 1.354(2) [1.357], C(1)–B(1): 1.640(3) [1.667], N(1)–P(1)–C(1): 87.31(8) [86.2].

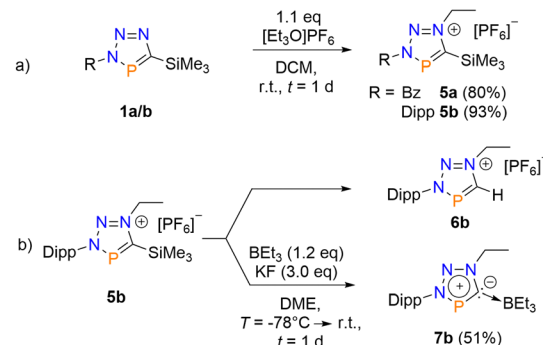
triazaphosphol-5-ylidene and thus as a phosphorus congener of the known tetrazol-5-ylidene with an abnormal substitution pattern (F, Scheme 1).<sup>11</sup> Moreover, **4a/b** is again isoelectronic to the cationic part of the triazaphospholenium salt **D** (Fig. 1).

From a mechanistic point of view, **4a/b** is formed by elimination of  $\text{FSiMe}_3$  from **2a/b**, which initially forms the carbene intermediate, that subsequently reacts with the remaining  $\text{BF}_3$ . This would be in line with observations reported by Borozov and co-workers for 1-ethyl-3-methyl-1*H*-imidazolium  $\text{BF}_4^-$  (and respectively  $\text{PF}_6^-$ ), which results in the formation of the corresponding NHC-based  $\text{BF}_3$  and  $\text{PF}_5$  Lewis pairs under rather harsh conditions.<sup>15</sup> In this respect, **4a/b** are also related to the  $\text{GaCl}_3$  adducts of neutral tetrazaphospholes, reported by Schulz and co-workers.<sup>16</sup>

In case of the formation of **4a/b** the free carbene could not be observed spectroscopically, probably due to a rapid Lewis pair formation. However, the by-product  $\text{FSiMe}_3$  was detected by means of  $^1\text{H}$ -,  $^{19}\text{F}$ - and  $^{29}\text{Si}$ - $^1\text{H}$ -HMQC NMR spectroscopy and can easily be removed under vacuum. It is likely that the protonation of the carbene leads to the formation of **3a**. This would be in agreement with observation that 1,2,3-triazylidenes can undergo migration of an alkyl group, that is bound to the most nucleophilic nitrogen atom, to the carbene carbon atom, while the formation of a protodesilylated side-product is also observed.<sup>13</sup>

Because **3a** and **4a** are apparently formed by competing reactions, the isolated yields were moderate. We therefore anticipated targeted syntheses of both compounds. While other electrophiles, such as  $\text{CH}_3\text{I}$  or  $\text{CH}_3\text{OTf}$ , are not suitable for quaternization reactions at triazaphospholes, we chose triethyloxonium hexafluorophosphate instead. This indeed yielded the corresponding triazaphospholenium salts **5a/b** in good isolated yields (**5a**: 80%, **5b**: 93%, Scheme 3a). Compounds **5a/b** provide again characteristic signals in the  $^{31}\text{P}\{^1\text{H}\}$  NMR spectra at  $\delta$ (ppm) = 238.1 (**5a**) and  $\delta$ (ppm) = 249.0 (**5b**), respectively. Additionally, the introduced ethyl group shows typical signals in the  $^1\text{H}$  NMR spectra (**5a**:  $\delta$ (ppm) = 4.73 (q,  $J$  = 7.5 Hz), 1.74 (t,  $J$  = 7.3 Hz); **5b**:  $\delta$ (ppm) = 4.84 (q,  $J$  = 7.1 Hz), 1.69 (t,  $J$  = 7.1 Hz)).

We also anticipated that the addition of potassium fluoride (KF) in the presence of a Boron-based Lewis acid  $\text{BR}_3$  should facilitate the formation of  $\text{FSiMe}_3$  and the abnormal carbene  $\rightarrow$   $\text{BR}_3$  adduct, while  $\text{K}[\text{PF}_6]$  might precipitate from the solution.



**Scheme 3** Synthesis of the triazaphospholenium salts **5a/b** (a). Preparation of the  $\text{BEt}_3$ -adduct **7b** and the protodesilylated compound **6b** (b).

For this purpose,  $\text{BH}_3\cdot\text{SMe}_2$ ,  $\text{BH}_3\cdot\text{THF}$ ,  $\text{BF}_3\cdot\text{SMe}_2$ ,  $\text{BF}_3\cdot\text{OEt}_2$ , and  $\text{BEt}_3$ , were used in combination with **5b**. Interestingly, except for  $\text{BEt}_3$ , the selective formation of the protodesilylated product **6b** was observed, most likely due to contaminations with  $\text{H}_2\text{O}/\text{HF}$ . On the other hand, in the presence of  $\text{BEt}_3$ , the  $\text{BEt}_3$ -adduct **7b** was selectively formed (Scheme 3b). This was confirmed by an X-ray structural analysis (Fig. 3). Compound **6b** was also independently synthesized and characterized crystallographically (see Table S4, ESI<sup>†</sup>).

Finally, we investigated the nature of the  $\text{C}_{\text{carb}} \rightarrow \text{B}$  bond by means of DFT calculations at the B3LYP-D3(BJ)/def2-SVP level of theory (see ESI<sup>†</sup> for details). We were particularly interested in the effect of the phosphorus atom on the donor–acceptor abilities of the abnormal carbene moiety.<sup>17</sup> The optimized structures are in good agreement with the experimentally measured ones (Fig. 2, 3 and Table S3 and Fig. S43, ESI<sup>†</sup>), with the  $\text{C}_{\text{carb}}\text{–B}$  bond lengths being slightly longer than those observed experimentally (**4a** 1.667 Å and **4b** 1.668 Å). The natural bond orbital analysis (Table S6 and Fig. S44, ESI<sup>†</sup>) indicates a strong donation of electrons as the  $\text{BF}_3$  bears a negative partial charge of  $-0.47$  (**4a**) and  $-0.46$  (**4b**). The Wiberg bond orders indicate a single bond character with 0.71 au in **4a** and **4b**. The Bader topological analysis<sup>18</sup> reveals an electron accumulation between the carbene carbon atom and the boron atom with a bond critical point that possesses a

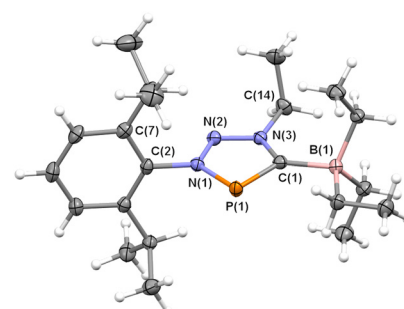


**Fig. 3** Molecular structure of **7b** in the crystal. Displacement ellipsoids are shown at the 50% probability level. Only one independent molecule in the asymmetric unit is shown. Selected bond lengths (Å) and angles (°): P(1)–C(1): 1.7306(10), P(1)–N(1): 1.7110(9), N(1)–N(2): 1.3146(12), N(2)–N(3): 1.3310(12), N(3)–C(1): 1.3629(13), C(1)–B(1): 1.6468(15), N(1)–P(1)–C(1): 88.26(4).



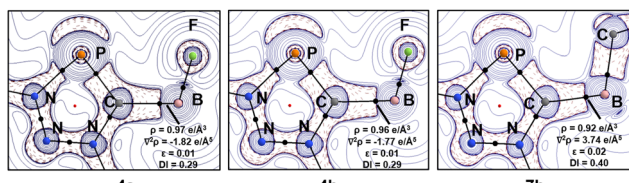


Fig. 4 Laplacian distribution of the electron density of compounds **4a/b** and **7b** (B3LYP-D3(BJ)/def2-TZVP//B3LYP-D3(BJ)/def2-SVP). Contour line diagrams of the Laplacian distribution  $\nabla^2\rho(r)$  in the PHC ring plane. Dashed red lines indicate areas of charge concentration ( $\nabla^2\rho(r) < 0$ ) while solid blue lines show areas of charge depletion ( $\nabla^2\rho(r) > 0$ ). The thick solid lines connecting the atomic nuclei are the bond paths and the small dots are the critical points. Bond Critical Points (in black), Ring Critical Points (in red).

relatively small electron density value ( $\rho(r)$ )  $0.97 \text{ e } \text{\AA}^{-3}$  **4a**,  $0.96 \text{ e } \text{\AA}^{-3}$  **4b**, and  $0.92 \text{ e } \text{\AA}^{-3}$  **7b**) with negative Laplacian values of  $\nabla^2\rho(r) = -1.82 \text{ e } \text{\AA}^{-5}$  (**4a**) and  $\nabla^2\rho(r) = -1.77 \text{ e } \text{\AA}^{-5}$  (**4b**), respectively a positive value of  $\nabla^2\rho(r) = 3.74 \text{ e } \text{\AA}^{-5}$  for **7b** (Fig. 4). Additionally, we have performed energy decomposition analysis (EDA-NOCV)<sup>19</sup> to quantitatively assess the chemical bonding situation in these adducts, taking as fragments the neutral triazaphosphol-5-ylidene (**4a/b**, **7b**) and  $\text{BF}_3$  moieties (Table S7 and Fig. S45, ESI<sup>†</sup>). The bond dissociation energy is slightly weaker than in other borane adducts, with energies of  $38.4$  (**4a**),  $37.5$  (**4b**) and  $40.0$  (**7b**)  $\text{kcal mol}^{-1}$ .<sup>20</sup> However, the dissection into preparation energy and interaction energy suggests that the geometrical deformation of  $\text{BF}_3$  or  $\text{BEt}_3$  brings a significant energy penalty ( $31.0$  and  $26.0 \text{ kcal mol}^{-1}$ ).

The interaction energy is comparable to other known  $\text{C}_{\text{carbene}} \rightarrow \text{B}$  adducts, counting  $-72.1$  (**4a**),  $-70.7$  (**4b**) and  $-68.4$  (**7b**)  $\text{kcal mol}^{-1}$ .<sup>21</sup> Further decomposition reveals an ionic nature of the bond with approximately 53% electrostatic interaction and 45% orbital interaction. Note that the electrostatic interaction refers to the electrostatic attraction between the charge distribution of the fragments, differentiating from the VB ionic bonds (for further details see ref. 20). The orbital term can be analysed with the Natural Orbitals for Chemical Valence (NOCV), where the  $\sigma$ -donation counts for  $\sim 80\%$  of the orbital interaction, while the  $\pi$ -back donation is only  $\sim 5\%$ . Fig. S46 (ESI<sup>†</sup>) shows a comparison of the frontier molecular orbital energies of the model systems 1,2,3-triazolylidene, tetrazol-5-ylidene and triazaphosphole-5-ylidene.

The energy of the  $\sigma$ -lone pair on the carbene carbon atom is comparable to the triazole analogue and agrees with the strong donor properties towards  $\text{BF}_3$  or  $\text{BEt}_3$ . On the other hand, the presence of a phosphorus atom provides less stabilization of the  $\pi^*$  orbital, leading to relatively high  $\pi$ -acceptor properties.

In summary, we have found an access to  $\text{BF}_3$  adducts of hitherto unknown triazaphosphol-5-ylidenes, which are the phosphorus analogs of tetrazol-5-ylidene carbenes with abnormal substitution pattern. Quantum chemical calculations reveal a strong  $\sigma$ -donor property and marginal  $\pi$ -accepting ligand properties. The access to transition metal complexes containing our novel triazaphosphole-5-ylidenes as ligands are currently performed in our laboratories.

Financial support provided by Freie Universität Berlin and the Deutsche Forschungsgemeinschaft (DFG) are gratefully acknowledged. D. M. Andrada thanks Prof. Dr. David Scheschkeiwitz and the University of Saarland for generous support.

## Conflicts of interest

There are no conflicts to declare.

## Notes and references

- (a) *Phosphorus: The Carbon Copy: From Organophosphorus to Phospho-Organic Chemistry*, ed. K. B. Dillon, F. Mathey and J. F. Nixon, John Wiley & Sons, 1998; (b) J. A. W. Sklorz and C. Müller, *Eur. J. Inorg. Chem.*, 2016, 595.
- L. Nyulászi, T. Veszprémi, J. Réffy, B. Burkhardt and M. Regitz, *J. Am. Chem. Soc.*, 1992, **114**, 9080.
- (a) Y. Y. C. Yeung Lam, Ko, R. Carrié, A. Muench and G. Becker, *J. Chem. Soc., Chem. Commun.*, 1984, 1634; (b) W. Rösch and M. Regitz, *Angew. Chem., Int. Ed. Engl.*, 1984, **23**, 900.
- (a) S. L. Choong, A. Nafady, A. Stasch, A. M. Bond and C. Jones, *Dalton Trans.*, 2013, **42**, 7775; (b) S. L. Choong, C. Jones and A. Stasch, *Dalton Trans.*, 2010, **39**, 5774.
- J. A. W. Sklorz, S. Hoof, N. Rades, N. De Rycke, L. Könczöl, D. Szieberth, M. Weber, J. Wiecko, L. Nyulászi, M. Hissler and C. Müller, *Chem. – Eur. J.*, 2015, **21**, 11096.
- L. Dettling, M. Papke, J. A. W. Sklorz, D. Buzsáki, Z. Kelemen, M. Weber, L. Nyulászi and C. Müller, *Chem. Commun.*, 2022, **58**, 7745.
- M. Papke, L. Dettling, J. A. W. Sklorz, D. Szieberth, L. Nyulászi and C. Müller, *Angew. Chem., Int. Ed.*, 2017, **56**, 16484.
- G. Guisado-Barrios, J. Bouffard, B. Donnadieu and G. Bertrand, *Angew. Chem., Int. Ed.*, 2010, **49**, 4759.
- M. H. Habicht, F. Wossidlo, T. Bens, E. A. Pidko and C. Müller, *Chem. – Eur. J.*, 2018, **24**, 944.
- M. Blug, O. Piechaczyk, M. Fustier, N. Mézailles and P. Le Floch, *J. Org. Chem.*, 2008, **73**, 3258; Y. Hatanaka and T. Hiyama, *J. Org. Chem.*, 1988, **53**, 918.
- (a) W. P. Norris and R. A. Henry, *Tetrahedron Lett.*, 1965, **17**, 1213; (b) J. Müller, K. Öfele and G. Krebs, *J. Organometal. Chem.*, 1974, **82**, 383; (c) L. Schaper, X. Wei, P. J. Altmann, K. Öfele, A. Pöthig, M. Drees, J. Mink, E. Herdtweck, B. Bechlars, W. A. Herrmann and F. E. Kühn, *Inorg. Chem.*, 2013, **52**, 7031.
- (a) W. J. Transue, A. Velian, M. Nava, M. A. Martin-Drumel, C. C. Womack, J. Jiang, G. L. Hou, X. Bin Wang, M. C. McCarthy, R. W. Field and C. C. Cummings, *J. Am. Chem. Soc.*, 2016, **138**, 6731; (b) T. E. Gier, *J. Am. Chem. Soc.*, 1961, **83**, 1769; (c) E. S. Yang, A. Mapp, A. Taylor, P. D. Beer and J. Goicoechea, *Chem. – Eur. J.*, 2023, e202301648; T. Görlich, D. Frost, N. Boback, N. T. Coles, B. Dittrich, P. Müller, W. D. Jones and C. Müller, *J. Am. Chem. Soc.*, 2021, **143**, 19365.
- (a) G. Guisado-Barrios, J. Bouffard, B. Donnadieu and G. Bertrand, *Angew. Chem., Int. Ed.*, 2010, **49**, 4759; (b) J. Bouffard, B. K. Keitz, R. Tonner, G. Guisado-Barrios, G. Frenking, R. H. Grubbs and G. Bertrand, *Organometallics*, 2011, **30**, 2617.
- A. J. Arduengo III, F. Davidson, R. Krafczyk, W. J. Marshall and R. Schmutzler, *Monatsh. Chem.*, 2000, **131**, 251.
- C. Tian, W. Nie, M. V. Borzov and P. Su, *Organometallics*, 2012, **31**, 1751.
- A. Villinger, P. Mayer and A. Schulz, *Chem. Commun.*, 2006, 1236.
- D. Munz, *Organometallics*, 2018, **37**, 275.
- R. F. W. Bader, *Atoms in Molecules: A Quantum Theory*, Clarendon, Oxford, 1990.
- L. Zhao, M. von Hopffgarten, D. M. Andrada and G. Frenking, *WIREs Comput. Mol. Sci.*, 2018, **8**, e13450.
- S. Dutta, S. M. De, S. Bose, E. Mahal and D. Koley, *Eur. J. Inorg. Chem.*, 2020, 638.
- (a) A. Krapp, F. M. Bickelhaupt and G. Frenking, *Chem. – Eur. J.*, 2006, **12**, 9196; (b) I. Fernández, N. Holzmann and G. Frenking, *Chem. – Eur. J.*, 2020, **26**, 14194; (c) L. Zhao, S. Pan and G. Frenking, *J. Chem. Phys.*, 2022, **157**, 034105.

